doi.org/10.52866/esj.2021.01.18.08

Calculation of Alpha Particles Track Parameters using Program Written by MATLAB Software (TRIAC)

Abdulqadher Makki Dahham1,a , Nada Farhan Kadhim1,b
Mustansiriyah University / College of Science - 1Department of Physics

Abstract

A new program was designed and written utilizing MATLAB software to perform image processing operations for the alpha particles tracks incident on the CR-39 nuclear tracks detector. The output code, named TRIAC, is using with connected digital camera as in Microscope (binocular) to obtained tracks picture. The program has been developed to calculate the track number, track density, and measure the track diameter (major axis, minor axis and equivalent axis). This developed code saves a lot of effort compared to the traditional manual method that usually use in the nuclear track's estimations. Besides that, it increases the accuracy of diameters measurement by avoiding the manual errors resulting from the use of the microscope.

Keywords: Computer image processing, CR-39 detector, Track density, Track diameter, Etching time, MATLAB.

حساب معلمات اثار جسيمات الفا
باستخدام برنامج أل(TRIAC) المكتوب بلغة الـ MATLAB

عبد القادر مكي دحام ، د.ندى فرحان كاظم
الجامعة المستنصرية / كلية العلوم - قسم الفيزياء

الخلاصة:

في العمل الحالي ، تم تصميم برنامج وكتابته باستخدام برنامج MATLAB لإجراء عمليات معالجة الصور لجسيمات ألفا التي تقع في كاشف المسارات النووية CR-39.

تم استخدام رمز الإخراج ، المسمى TRIAC ، مع كاميرا رقمية متصلة بمجهر ضوئي لغرض تصوير المسارات التي تم الحصول عليها. تم تطوير البرنامج لحساب عدد المسارات وكثافة المسار وقياس قطر المسار (المحور الرئيسي والمحور الثانوي والمحور المكافئ). يوفر هذا الكود المطور الكثير من الجهد مقارنة بالطريقة اليدوية التقليدية التي تستخدم عادةً في تقديرات المسارات النووية. إلى جانب ذلك ، فإنه يزيد من دقة قياس الأقطار عن طريق تجنب الأخطاء اليدوية الناتجة عن استخدام المجهر.

الكلمات المفتاحية: معالجة الصور، كثافة المسار ، قطر المسار ، كاشف الاثر MATLAB ، CR-39.

INTRODUCTION

Solid-State Nuclear Track Detectors (SSNTDs) have a wide application in many fields of radiation science and technology. There are a lot of types of these detectors [1-11]. CR39 (Columbia Resin-39) is one of these detectors with a thermoset plastic which is a polymeric form of diethylene glycol bis (allyl carbonate) [4]. The efficacy of different types of nuclear impact reagents in being sensitive to the particles depends on the type and energy of the falling particle [19, 20]. Although electronic detectors have better properties in detecting the type and energies of the particles , resorting to the use of plastic detectors such as (CR-39, CN-85, LR-115) may be more appropriate in some applications to monitoring the radioactive contamination, [5,6,7,8] due to easy to use and their lack of need for electronic devices and power supplies. Although, SSNTDs haven't ability to distinguish the different energies but they have a very high detection efficiency approaching 100%. As most or all of the material particles, such as protons, alpha particles, and ions that fall on detectors materials lead to the formation of stable traces in these detectors [9,10,12,13]. The decisive factors in determining the accuracy of the measurements, this enumeration process is usually done manually by using an ordinary optical microscope in determining the number of traces per unit area for the detector. This process of the diameter measuring known as a manual method [21,22]. This method requires significant human effort in addition to the potential for errors during the counting and measurement processes. A damage region is created due to the passing of a charged particle through the SSNTD material and it is known as the latent track. By applying an appropriate etchant (i.e., NaOH or KOH), latent tracks can be etched sufficiently enlarging them to become visible under an optical microscope (with diameters of 1 μm or more). Utilizing the suitable apparatus one can take images of the SSNTDs surface and count track numbers [14, 15, 16,17].

The tracks occur in detectors materials when exposed to alpha source as example; depend on the incident alpha energy. In such case, the alpha range in any medium depends on density of medium you can determine it, by depend on the equation (1). [18]:

$$R = 0.318\, E^{1.5} \tag{1}$$

where R is the range of alpha in the medium in (cm) and E is the energy of the alpha particle in (Mev) Further, energy value as a function of range can be written as:

$$E = 2.146R^{0.6667} \quad (2)$$

Using above relation, the residual energy at distance x from the source can be now computed as:

$$E = 2.146\,(R - x)^{0.6667} \quad (3)$$

The aim of the present work is to write a computer program with Matlab2012 to count alpha radiation tracks formed on the surface of the CR-39 detector, and measure their diameters (large axis, small axis and equivalent axis).

EXPERIMENTAL METHODS

In the present work, CR-39 detector is used as example of wide used SSNTDs. The thickness of used CR-39 detector is 500μm and supplied by "Pershore Molding LTD Co. UK." Cutting with dimension of ($1cm^2$) [4].

For experimental work, group of CR-39 nuclear track detectors were exposed for 5 sec to radium source Ra-226 as alpha particles emitter (energy=5.49 Mev with 4.08 cm average range in air) [23]. Ra-226 source activity is 5μci with uncertainty 6% (k=2).

The distances between the source and the detector have been changed to get several energy radiations. A hand-made tool, as showing in Fig (1), is used to change the distance between source and detectors. This tool let only the direct incident particles reach to the detectors through a small hall. The used distances were 0,1,2,3, and 4 cm to get energies 5.49, 4.542, 3.508, 2.272, and 0.430 MeV respectively. Equation 3 is used to calculate the energy.

The exposed detectors are etched for 60, 120, 180, and 240 min with NaOH solution with normality of 6.25 N and temperature 60 C°. After etching, the tracks on detectors were viewing and counted with optical microscope (Novel) model: N-200M, supplied with a digital camera to viewing tracks and save photo to use it in the developed MATLAB program code to count the tracks and measure the diameter.

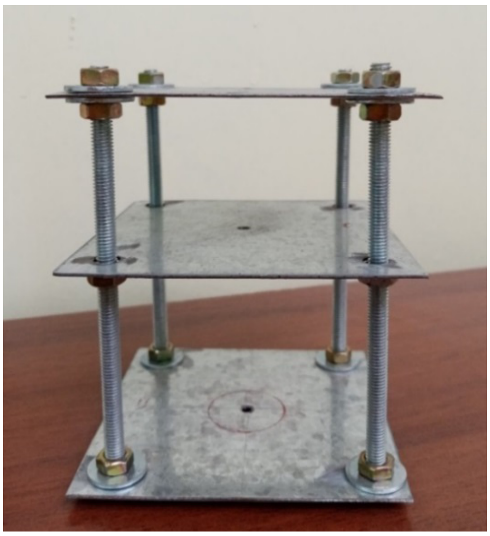

Figure (1) hand-made tool use to espouse the detector with different energy by changing the distances between the source and the detector.

Computer image processing

A computer program code was written and developed in Matlab2012 to count tracks formed on the surface of the CR-39 detector and measure their diameters (large axis, small axis and equivalent axis) in addition to circumference tracks. This presented program code is named (TRACK). To establish this code, Matlab›s sensitive functions as a function of gray color and the image turns gray until the program senses the nuclear tracks are used. The images are processed by the program, and converted into a binary image as shown in Figure (2). In this case the program can isolate tracks from defects. In such case, the treatment process, the counting and calculations take only a few seconds with more precisely and accuracy compared to traditional (manual) method with personal counting depending on eyes and measuring scale.

The tracks censuses showed a good agreement between the two methods computational and manual. While the precision in diameters measuring is much superior for computer method compare to the manual counterpart. As the resolution of the first is in the limits of pixels, in order to ensure the correct performance and efficiency of the program, it has been completed make a comparison of the data obtained by using the program and those obtained by the manual method.

After the program establishment and verification correctly with the manual results, now the program correctness is quite sufficient for operation. Different pictures of different tracks and different etching time when exposed detectors to alpha particle of energy 4.552 Mev were taken and shown in Figure (3). The diameters at the beginning of the etching process are small but in the advanced stages of the etching process these diameters increase successively.

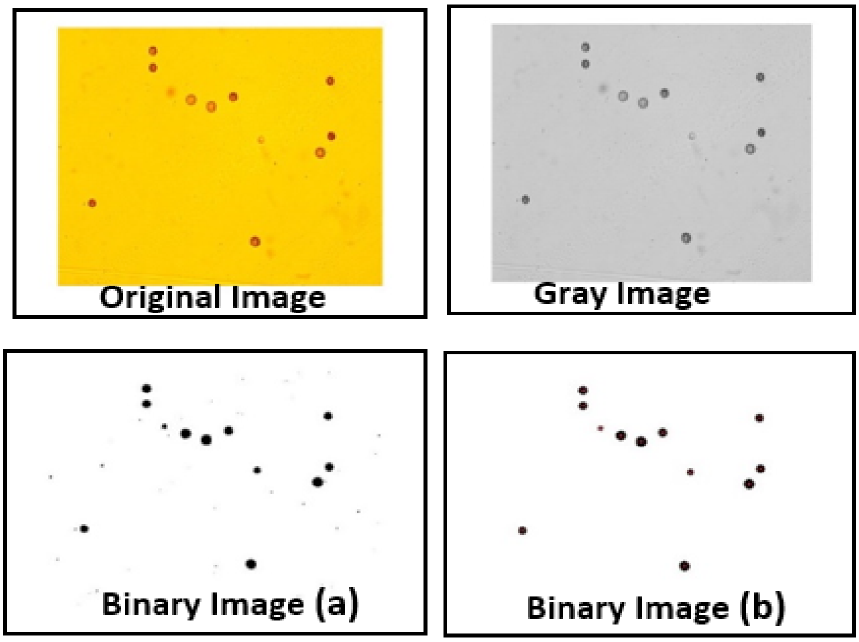

Figure 2 The four main steps of track image analysis. The resulting corrected binary image (b) is finally used for counting the tracks.

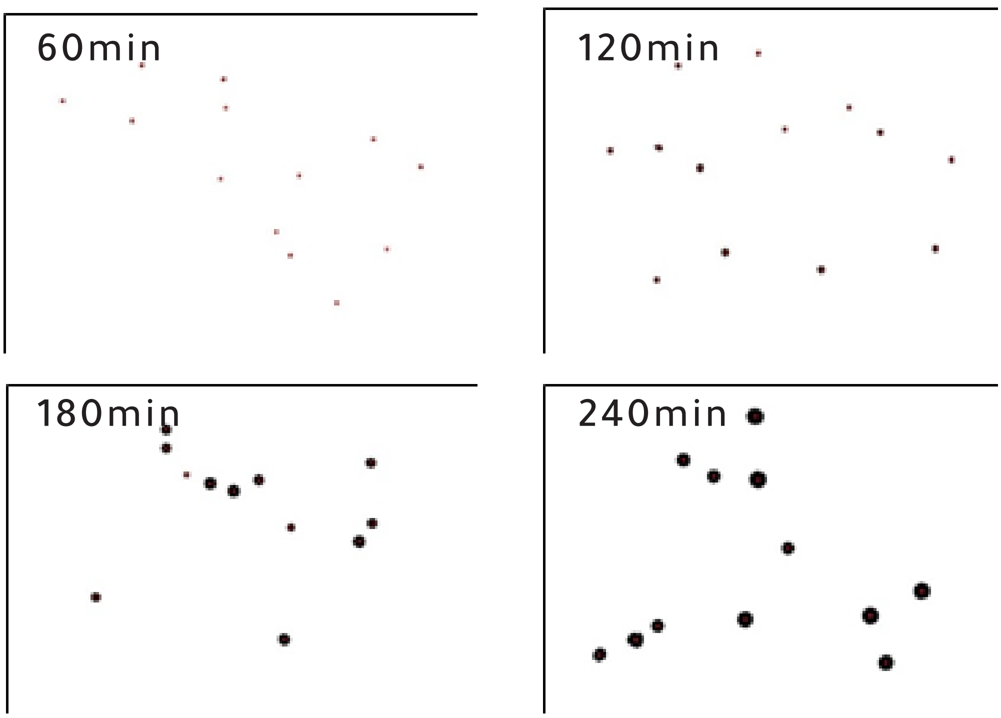

Figure 3 binary image for different etching time (1, 2, 3,4hr) at alpha energy (4.552Mev)

RESULTS AND DISCUSSIONS

The developed computer program code, after verify its performance, was used to count tracks and measure its diameters at different etching times and particle alpha energy emitted from the radium source Ra-226.

The results that obtained for track density at different etching time with the developed code are tabulated in tables (1, 2, 3, and 4).

Tables 1, 2, 3, and 4 present the etching time (min) with the track density and diameter relative to the alpha energies 4.552, 3.508, 2.272, and 0.430 Mev respectively. It's obvious that the optimum track density is developed at etching time of 2 hours (120 min), whereas after this time the number of the tracks was decreased. This decreases due to the overlap of tracks.

Table 1 the etching time with the developed track density and diameter for the alpha energy of (4.552 Mev).

Etching Time (min)	Track Density (track/mm^2)	diameter axis (µm)		
		Large axis	Small	Equivalent
60	221	2.74	1.92	2.51
120	272	5.11	4.83	4.90
180	204	7.78	7.58	7.66
240	198	11.66	11.24	11.43

Table 2 the etching time with the developed track density and diameter for the alpha energy (3.508 Mev).

Etching Time (min)	Track Density (track/ mm^2)	diameter axis (µm)		
		Large	Small	Equivalent
60	204	2.46	2.18	2.24
120	238	4.91	4.44	4.65
180	192	7.36	6.96	7.14
240	187	11.24	10.80	11.01

Table 3 the etching time with the developed track density and diameter for the alpha energy (2.272 Mev).

Etching Time (min)	Track Density (track/ mm^2)	diameter axis (µm)		
		Large	Small	Equivalent
60	170	2.34	1.83	2.00
120	188	5.25	4.07	4.55
180	122	7.86	6.15	6.82
240	102	12.22	10.21	10.43

Table 4 the etching time with the developed track density and diameter for the alpha energy (0.430 Mev).

Etching Time (min)	Track Density (track/ mm^2)	diameter axis (µm)		
		Large	Small	Equivalent
60	120	2.40	1.59	1.73
120	144	3.99	3.62	3.74
180	68	7.14	5.66	6.26
240	68	10.99	9.86	10.39

This is true for all exposed energy except (0.430) Mev which is achieved at 4cm distance, because the number of the latent tracks recorded in the detector at this energy were very little, where the short range of alpha let only little number of particles can reach the detector at 4 cm. Therefore, after 2h the etching time increases, the diameter of the tracks can increase but their number increase because of the little number of the tracks which cannot overlap each other.

Table (1, 2,3, and4) showed that the highest density of the tracks would be for the 1cm between the source and the detector i.e. at1cm where the energy of the source has its initial value (4.552Mev), it was 272at the optimum etching time (2h), while it decreased to 144 at 4cm distance (0.430Mev) at the same etching time.

It's also clear that the density of the tracks has direct relationship with alpha energy. Whenever the energy decreased, the density of the tracks decreased. The track density variation at different etching time f (60, 120, 180, and 240 h) relative to the alpha energy (4.552, 3.508, 2.272, 0.430 Mev) are presented in Figure (4). 2 h is the best etching time with maximum track density. Figure (5) illustrates the relation between the track diameters and the etching time relative to alpha energies. Increasing in the track diameter relative to the increasing in the etching time is obvious for all alpha energies.

Figure 4.
track density relative the four-etching time for the energy of the incident alpha particle. (4.542, 3.508, 2.272, 0.430 Mev).

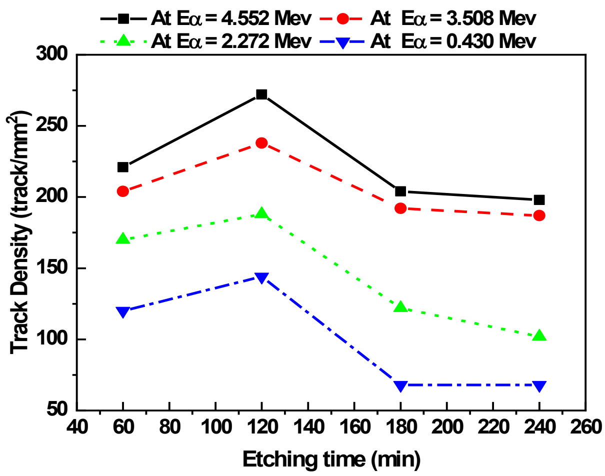

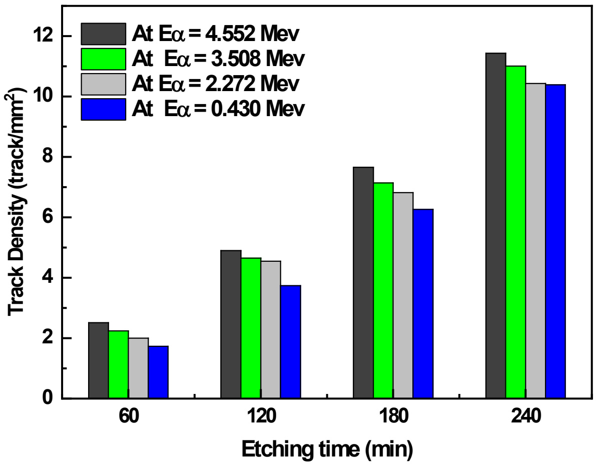

Figure 5.
Track diameter relative to the etching time for the alpha energy (4.552, 3.508, 2.272, 0.430 Mev).

Conclusions:

Results conclude the following points:

1. The written program presented in this paper provides added speed and accuracy in operations count tracks and measures their diameters.
2. The new programming is very fast in calculating the number of tracks on the surfaces of the nuclear detector compared to Manual (traditional) method.
3. As for accuracy, the digital pixel dimensions provide superior resolution several times the accuracy obtained by hand.
4. It is crucial to take into account the detector when cutting and scraping from scratching or the effect of that because some scratches or impurities are of the effect size, so the program will be calculated as tracks. These impurities can be avoided by manipulating the threshold limit of the program to be deleted without affecting on the results.

Acknowledgements

Authors would like to thank the radiation laboratory staff, Department of Physics, College of Science, Mustansiriyah University for their support. Special thanks to assistant professor Murtaza Fayez for providing us his insight and expertise that greatly assisted this research.

References

[1] Kadhim, Y. A., Kadhim, N. F., & Ibrahim, N. K. (2019). Determination of Alpha Rates Emitted from Animal Bones Using CN-85 Nuclear Track Detector. American Journal of Quantum Chemistry and Molecular Spectroscopy, 3(1), 7-11.

[2] Fleischer, R. L., Price, P. B., Walker, R. M., & Walker, R. M. (1975). Nuclear tracks in solids: principles and applications. Univ of California Press.

[3]. D. Palacios, F. Palacios, E. M. Yushimura, G. Palacios and A. A. R. Da Silva, J. Radioanal. Nucl. Ch. 307 793-799 (2016).

[4] Kadhim, N. F., Ridha, A. A., Salim, M. D., Hanfi, M. Y., & Mostafa, M. Y. (2021). Development of alpha tracks measurement with thermal oven as an etching technique for SSNTDs. Materials Today: Proceedings.

[5] Al-Jubbory, M.M.S. (2004), MSc. Thesis, Physics Department, College of Education, University of Mosul, Iraq.

[6] Nikjoo, H., Uehara, S., & Emfietzoglou, D. (2012). Interaction of radiation with matter. CRC press.

[7] Al-Jumaely, F.M.A. (2009), PhD. Thesis, Physics Department, College of Science, University of Mosul, Iraq.

[8] Yu, K. N., Ng, F. M. F., & Nikezic, D. (2005). Measuring depths of sub-micron tracks in a CR-39 detector from replicas using Atomic Force Microscopy. Radiation measurements, 40(2-6), 380-383.

[9] Al-Jubbori, M.A.D. (2004), PhD. Thesis, Physics Department, College of Education, University of Mosul, Iraq.

[10] Patiris, D. L., Blekas, K., & Ioannides, K. G. (2007). TRIAC II. A MatLab code for track measurements from SSNT detectors. Computer physics communications, 177(3), 329-338.

[11] Sinenian, N., Manuel, M. E., Zylstra, A. B., Rosenberg, M., Waugh, C. J., Rinderknecht, H. G., ... & Johnson, M. G. (2012). Upgrade of the MIT Linear Electrostatic Ion Accelerator (LEIA) for nuclear diagnostics development for Omega, Z and the NIF. Review of Scientific Instruments, 83(4), 043502.

[12] Patiris, D. L., Blekas, K., & Ioannides, K. G. (2006). TRIAC: A code for track measurements using image analysis tools. Nuclear Instruments and Methods in Physics Research Section B: Beam Interactions with Materials and Atoms, 244(2), 392-396.

[13] Fews, A. P. (1992). Flexible analysis of etched nuclear particle tracks. Nuclear Instruments and Methods in Physics Research Section B: Beam Interactions with Materials and Atoms, 72(1), 91-103.

[14] Molnar, J., Somogyi, G., Szilagyi, S., & Sepsy, K. (1984). Development of a CCD based system called digitrack for automatic track counting and evaluation. Nuclear Tracks and Radiation Measurements (1982), 8(1-4), 243-246.

[15] Skvarc, J. (1993). Automatic image analysis system TRACOS. Informacije Midem, 23(3).

[16] Boukhair, A., Haessler, A., Adloff, J. C., & Nourreddine, A. (2000). New code for digital imaging system for track measurements. Nuclear Instruments and Methods in Physics Research Section B: Beam Interactions with Materials and Atoms, 160(4), 550-555.

[17] Young, D. A. (1958). Etching of radiation damage in lithium fluoride. Nature, 182(4632), 375-377.

[18] Bataller, G., & Girard de Vasson, O. (1989). Use of nuclear track detector to measure very low alpha radioactiv-

ity in urine. Radiation Protection Dosimetry, 26(1-4), 217-221
[19] Nicholas, T. (1995). Measurement and detection of radiation.
[20] Ahlen, S. P. (1980). Theoretical and experimental aspects of the energy loss of relativistic heavily ionizing particles. Reviews of Modern Physics, 52(1), 121.
[21] Kadhim, N. F., & Jebur, L. A. (2018). Investigation of the favorable etching time of CN-85 nuclear track detector. Applied Radiation and Isotopes, 135, 28-32.
[22] García, V., Palacios, D., & Sajo-Bohus, L. (2016, July). New approach to determine the incident alpha energy and angle from track parameters. In AIP Conference Proceedings (Vol. 1753, No. 1, p. 080008). AIP Publishing LLC.
[23] S.A, Durrani, and R, Ilić, Radon (1997). Measurements by etched track detectors (World Scientific, Singapore).

TRACK CODE

```
clc;close all;clear all;

[FNm، fldr] = uigetfile({'٭.BMP';'٭.png';'٭.JPG';'٭.bmp';'٭.tif'});
٪[FNm، fldr] = uigetfile({'٭.bmp';'٭.png';'٭.JPG';'٭.tif'});
fm = fullfile(fldr، FNm);
Lx=0.28; ٪mm
Ly=0.21; ٪mm
Am=Lx٭Ly

I0=imread(fm);
[py px tt]=size(I0);
scfx=Lx /px;
scfy=Ly /py;

I1=rgb2gray(I0);
٪ th=0.5٪٪٪٪٪٪٪٪٪٪٪٪٪٪٪٪
th=0.67; BW=im2bw(I1،th);
٪٪٪٪٪٪٪٪٪٪٪٪٪٪٪٪٪٪٪٪٪٪٪٪٪٪
٪figure، imshow(I0);
٪figure، imshow(BW);
SE = strel('square'،3); BW2 = imdilate(BW،SE);
٪٪٪٪٪٪٪٪٪٪٪٪٪٪٪٪٪٪٪٪٪٪٪٪٪٪٪٪٪٪٪٪٪٪٪٪٪٪٪
BW2 = ~imfill(~BW،'holes');
٪figure، imshow(BW2);

th1=500;
BW3 = ~bwareaopen(~BW2، th1);

st = regionprops(~BW3،'All');
centroids = cat(1،st.Centroid);

٪٪ ٪٪٪٪٪٪٪٪٪٪٪٪٪٪٪٪٪٪٪٪٪٪٪٪٪٪٪٪٪٪٪٪٪٪٪٪٪٪٪٪٪٪٪
٪٪٪٪٪٪٪٪٪٪٪٪٪٪٪٪٪
L1=[st.MajorAxisLength];
L2=[st.MinorAxisLength];
L3=[st.EquivDiameter];
Lp=[st.Perimeter];
A1=[st.Area];
٪٪ ٪٪٪٪٪٪٪٪٪٪٪٪٪٪٪٪٪٪٪٪٪٪٪٪٪٪٪٪٪٪٪٪٪٪٪٪٪٪٪٪٪٪٪
٪٪٪٪٪٪٪٪٪٪٪٪٪٪٪٪٪
Lc=L1. /L2;
Lpp=pi٭L3;
Lcp=Lpp. /Lp;
```

```
ci = (Lp .^2 ). / (4*pi*A1)
%% %%%%%%%%%%%%%%%%%%%%%%%%%%%%%%%%%%%%%%%%%%%%%%%%%%%%
%%%%%%%%%%%%%%%%%%%%
LG=25;x=1:LG;
mnc=min(ci);
mxc=max(ci);
mmc=mxc-mnc;
Ci=sort(ci);
Ci=round(LG*(Ci-mnc) /mmc)
% histgramcirclaurty
hc=hist(Ci،LG);

Cii=(x*mmc /LG+mnc);  % in mm*mm
cr1=0.6;
cr2=1.4;
Cx1=round(LG*(cr1-mnc) /mmc);

if Cx1<1 Cx1=1;end;
mmmm=(cr2-mnc) /mmc;

Cx2=round(LG*(cr2-mnc) /mmc);
if Cx2>25 Cx2=25;end;

smc=sum(hc)
suc=sum(hc(Cx1:Cx2))
rt_c=suc /smc
%% %%%%%%%%%%%%%%%%%%%%%%%%%%%%%%%%%%%%%%%%%%%%%%%%%%%%
%%%%%%%%%%%%%%%%%%%%
st
mxA=max(A1);
mnA=min(A1);
A=sort(A1)
mm=mxA-mnA;
A=round(LG*(A-mnA) /mm)

%%% Histogram Area

h2=hist(A،LG);

Amm=(x*mm /LG+mnA)*scfx*scfy;  % in
mm*mm
Amm
Ammc=Amm*1e6;
%% %%%%%%%%%%%%%%%%%%%%%%%%%%%%%%%%%%%%%%%%%%%%%%%%%%%%
%%%%%%%%%%
%fg1=figure('units'،'normalized'،'outerpositi
on'،[0 0 1 1]);
figure،;imshow(I0);
figure، imshow(I1);
%subplot(3،3،3);
figure،imshow(BW);%subplot(3،3،4);
figure،imshow(BW2)
%% %%%%%%%%%%%%%%%%%%%%%%%%%%%%%%%%%%%%%%%%%%%%%%%%%%%%
%%%%%%%%%%
%subplot(3،3،5);
figure،imshow(BW3);
hold on
%subplot(3،3،5);
%figure،
plot(centroids(:،1)،centroids(:،2)،'r*')
hold off
%% %%%%%%%%%%%%%%%%%%%%%%%%%%%%%%%%%%%%%%%%%%%%%%%%%%%%
%%%%%%%%%%
%subplot(3،3،7);
%hist(A);
%subplot(3،3،8); histgram area mm^2 area in
x
figure،plot(Amm،h2);
%subplot(3،3،9);
%cir with sequnce of spots in x squnce
number of spots & y =ci

figure،plot(ci);
hold on
cx=[0 33]; cy=[cr1 cr1];
plot(cx،cy،'r'،'LineWidth'،2);
hold on
cx=[0 33]; cy=[cr2 cr2];
plot(cx،cy،'r'،'LineWidth'،2);
hold off
%% %%%%%%%%%%%%%%%%%%%%%%%%%%%%%%%%%%%%%%%%%%%%%%%%%%%%
%%%%%%%%%%
```

```
٪subplot(3،3،2);

٪histgram ci with real Cir in x
figure،plot(Cii،hc);
٪٪
mcr=x٭scfx٭1e3;

Am=Lx٭Ly
SA=sum(A)
SAmm=SA٭scfx٭scfy
[hi wi]=size(BW);
TA=hi٭wi
RT=SA /TA

L1m=L1٭scfx٭1e3٪in mic٭r;
L2m=L2٭scfx٭1e3٪in mic٭r;
L3m=L3٭scfx٭1e3٪in mic٭r;
Lpm=Lp٭scfx٭1e3٪in mic٭r;
ML1=mean(L1m)
ML2=mean(L2m)
ML3=mean(L3m)
MLp=mean(Lpm)
```